Mangrove Forest Extraction from COSMO-SkyMed Second Generation X-band Multi-polarization Data

Chenghua Shi*, Ken Yoong Lee, Chenguang Hou, Kim Hwa Lim, Soo Chin Liew

Centre for Remote Imaging, Sensing and Processing, National University of Singapore.

10 Lower Kent Ridge Road

Blk S17, Level 2, Singapore 119076

*crssc@nus.edu.sg

Abstract: *Numerous studies have been conducted in mapping mangrove forests by using synthetic aperture radar (SAR) imagery. In this paper we employed a machine learning method, i.e., U-Net, for mangrove forest extraction from COSMO-SkyMed Second Generation (CSG) multi-polarization X-band SAR data. The selected study areas were located at Matang and Sungai Pulai in Peninsular Malaysia. A total of seven CSG quad-polarization scenes were acquired from 26th October 2022 to 23rd June 2023. To support the training of the U-Net, a cloud-free SPOT-6 pan-sharpened multispectral scene over Matang study site, which was captured on 9th March 2022, were annotated manually for both mangrove and non-mangrove classes. After speckle filtering and orthorectification, the enhanced ellipsoid corrected intensity components were used as inputs into the U-Net. The U-Net model was first trained with the CSG scene acquired on 26th October 2022 over Matang North area and then applied to the remaining six CSG scenes for performance evaluation. The mangrove forest extraction results from the CSG multi-polarization data showed that the overall accuracies were greater than 94%, except for those of Matang South area. In comparison, the overall accuracies of mangrove forest extraction from the CSG single-polarization data using a similarly trained U-Net model were greater than 92% on average.*

Keywords: *Mangrove forest, U-Net, COSMO-SkyMed Second Generation, X-band*

Introduction

Mangrove forests are salt-tolerant evergreen forest ecosystems that occur in coastal intertidal zones of tropical and subtropical areas (Islam et al., 2024; Romañach et al., 2018; Whitmore, 1984). By storing a considerable amount of carbon in the aboveground biomass and in marine sediments, mangrove forests are unique blue carbon systems and important regulators of climate change (Donato et al., 2011; Hamilton et al., 2018; Murdiyarso, 2015). Mangrove forests have attracted much research interest because of their various and sustainable ecosystem functions, such as providing coastal protection, serving as a haven for diverse terrestrial and marine fauna, being a booster of food security and livelihood support for coastal communities (Chong, 2006; Alongi et al., 2016; Wang et al., 2019). Currently, there exist some global records indicating a significant loss of mangrove forest cover in the past five decades due to human activities (Bunting et al., 2018; Friess et al., 2019). Hence, there is a critical need to monitor mangrove forest changes that can be done more accurately and on a large scale, for example, with the use of spaceborne remote sensing (Pham et al., 2019).

Many studies have been conducted for mapping mangrove forests by using remote sensing data (Abdel-Hamid et al., 2018; Chen et al., 2017, Ghorbanian et al., 2021; Jhonnerie et al., 2015; Liu et al., 2021; Lucas et al., 2014; Sharifi et al., 2022). Compared to electro-optical remote sensing, SAR imaging offers its advantages of independence of sunlight and weather conditions. In the literature, the use of C- and L-band for mangrove forest related applications was studied by Proisy et al. (2000), Hamdan et al. (2014), Kovacs et al. (2013), Vu et al. (2014), etc. To date, many X-band SAR satellites have been launched, such as COSMO-SkyMed, TerraSAR-X, KOMPSAT-5, NeuSAR, TeLEOS-2, DS-SAR and others. Therefore, it is of great interest to evaluate the capability of X-band SAR for mangrove forest extraction.

Study Areas

As indicated in Figure 1, two study areas in Peninsular Malaysia were selected, namely, Matang in Perak state and Sungai Pulai in Johor state. The first study site consists of Matang Mangrove Forest Reserve (MMFR), which is the largest mangrove forest reserve in Peninsular Malaysia with an area of approximately 40,000 hectares (Ong & Gong, 2013; Lucas et al., 2021). Due to the CSG scene coverage limitation, the MMFR is separated into two parts, which are hereafter called Matang North and Matang South. The Sungai Pulai Mangrove Forest Reserve (SPMFR), which is the largest riverine mangrove system in Johor, is the second study area. In 2003 about 9,126 hectares of the SPMFR was designated as a RAMSAR site (Kanniah et al., 2021; Mohd Hasmadi et al., 2011).

Figure 1: Location map of study sites

Methodology

a. Satellite Data Acquisition

COSMO-SkyMed (Constellation of Small satellites for Mediterranean basin Observation) is an Italian Earth Observation Space System operating at X-band (3.1 cm wavelength). Its second generation provides high-resolution quad-polarization data through two enhanced satellites, namely, CSG1 and CSG2. Being positioned separately at 180° on the same orbit, each CSG satellite has a revisit time of 16 days. For the CSG quad-polarization stripmap imaging mode, both azimuth and range resolutions are about three meters (Agenzia Spaziale Italiana, 2021). A total of seven CSG quad-polarization single-look complex (SLC) data were acquired in this study. Four of them were acquired over Matang North, two over Matang South, and one over Sungai Pulai. Figure 2 shows the CSG scenes over the selected study sites. The corresponding data specifications are summarized in Table 1.

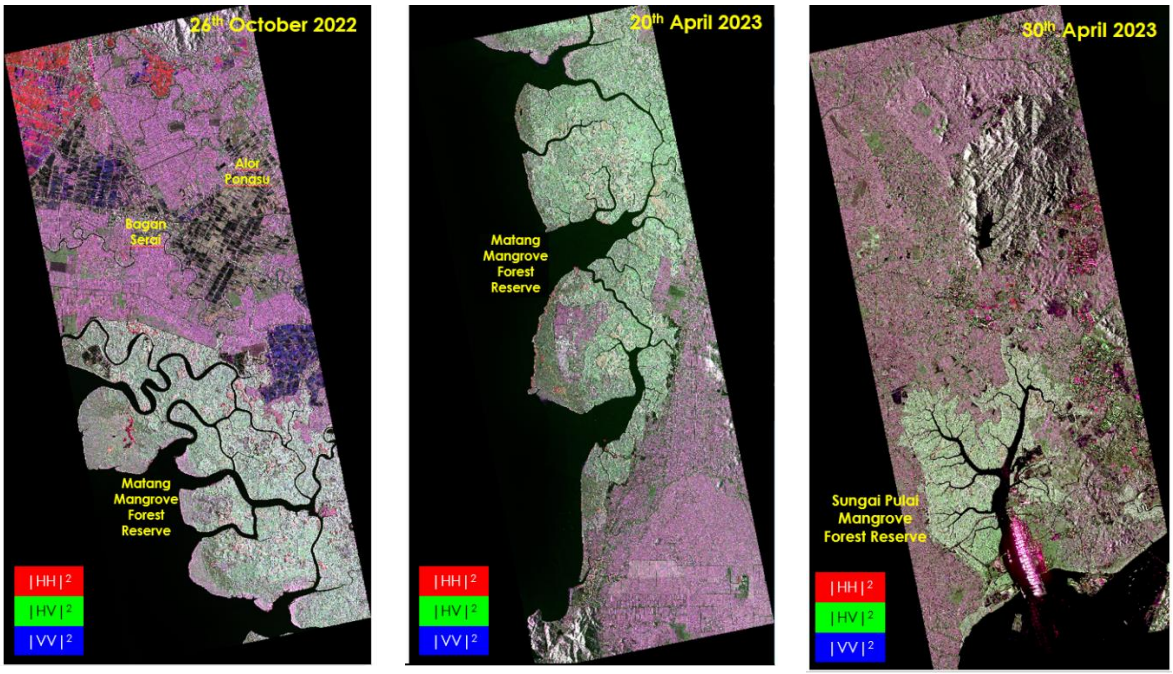

(a) (b) (c)

Figure 2: CSG scenes acquired over (a) Matang North, (b) Matang South, (c) Sungai Pulai

b. Data Annotation

In this study, data annotation was carried out on a pan-sharpened multispectral SPOT-6 scene over Matang. The SPOT-6 orthorectified scene was acquired on 9th March 2022 with a spatial resolution of 1.5 m. It was cut into tiles, each of 2048×2048 pixels. The SPOT-6 image tiles and annotations over the training region are displayed in Figure 3. A total of 164 tiles were

annotated. Some tiles were not annotated as they contained mainly water or belonged to a single class. The annotated tiles were used subsequently for U-Net training and accuracy assessment.

Table 1: Specifications of CSG test data

	Matang North	**Matang South**	**Sungai Pulai**
Acquisition date	26th October 2022 20th April 2023 22nd May 2023 23rd June 2023	20th April 2022 22nd May 2023	30th April 2023
Wavelength	X-band (~ 3.1 cm)		
Polarization	Quad-polarization (HH, HV, VH, VV)		
Satellite ID	SSAR1		
Satellite altitude	~ 625 km		
Orbit direction	Ascending		
Revisit time	16 days		
Imaging mode	Stripmap		
Beam number	QPS-020	QPS-020	QPS-015
Antenna direction	Right		
Product type	SGS_B		
Number of looks	1 (azimuth), 1 (range)		
Near range look angle	~ 38.74°	~ 38.74°	34.277°
Far range look angle	~ 39.57°	~ 39.57°	35.246°
Line spacing	2.233 m	2.233 m	2.153 m
Pixel spacing	1.499 m	1.499 m	1.285 m

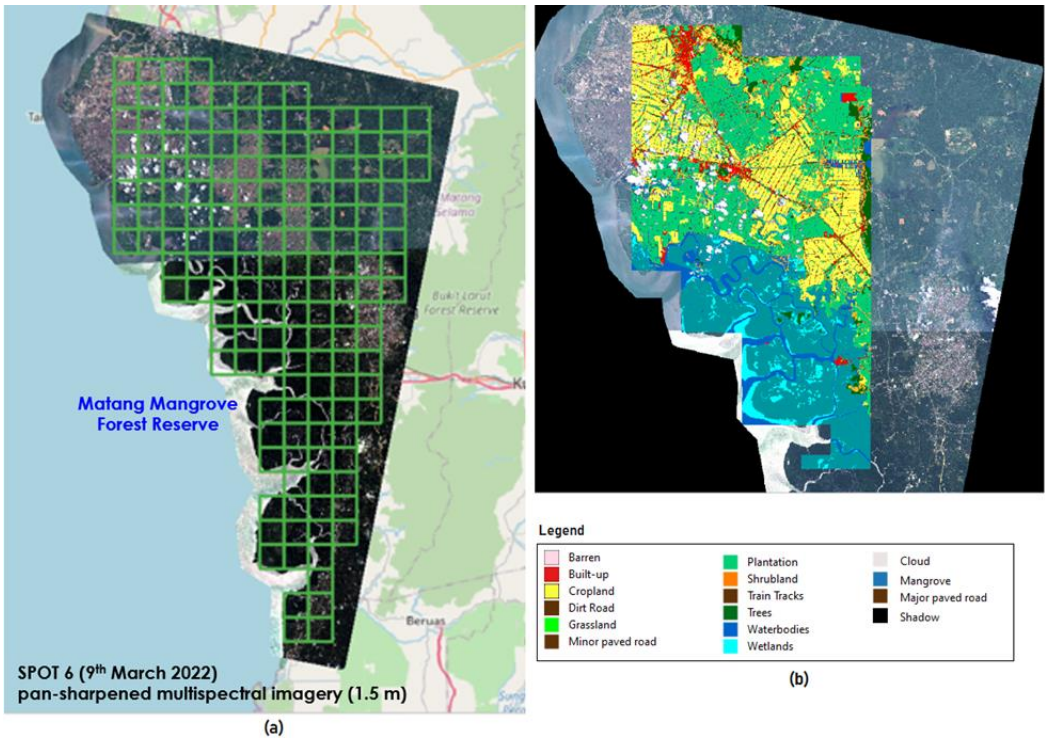

Figure 3: Data annotation: (a) 164 tiles of SPOT6 scene, (b) annotation over Matang North

c. Machine Learning

The U-Net was originally introduced by Ronneberger et al. (2015) for biomedical image segmentation. It is a deep encoder-decoder architecture, which is able to achieve high accuracy in pattern recognition with limited training data. Its application for land use land cover classification of remotely sensed images can be found in Solórzano et al. (2021).

Since the U-Net model can leverage effectively a smaller amount of data while maintaining high speed and accuracy, it was reasonably suitable for our purpose. There were only 164 annotation tiles, of which 136 tiles over Matang North were used for training. The structure of our U-Net model is illustrated in Figure 4. In this study, the CSG scene of Matang North acquired on 26th October 2022 was used for training the U-Net model. Mangrove and cloud classes were set separately to 1 and 255. Meanwhile, all the other classes were set to 0. In the multi-polarization model, the three input channels were HH, HV, and VV intensities, while the output channel contained only Mangrove and Non-mangrove classes. The window size of the model was 128×128 pixels and the CrossEntropyLoss function was used as the loss function. In each of the three single-polarization models, thethree input channels were all the same, from one of the HH, HV or VV intensity, respectively. The trained U-Net models were applied to the remaining six CSG scenes for mangrove forest extraction.

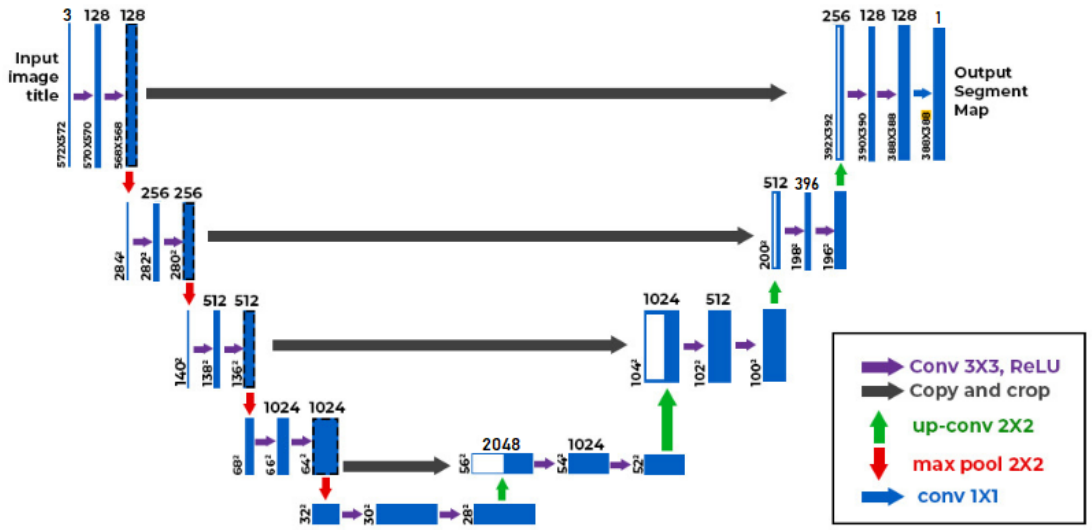

Figure 4: U-Net model used in mangrove forest extraction

d. Mangrove Forest Extraction

The entire processing workflow is illustrated in Figure 5. A total of seven CSG data were acquired during the period from 26th October 2022 to 23rd June 2023. During multi-looking, four-look intensity images were formed by taking two pixels in range direction and two pixels in azimuth direction from each SLC data. Note that the cross-polarized one was obtained by averaging HV and VH complex values. A two-iteration gravitational filter (Lee et al., 2021) with a 7×7 window was then applied to the intensity images. Subsequently, the speckle-filtered intensity images were orthorectified by using backward geocoding technique (Small & Schubert, 2018) with 30m Copernicus Global Digital Elevation Model (COP-DEM).

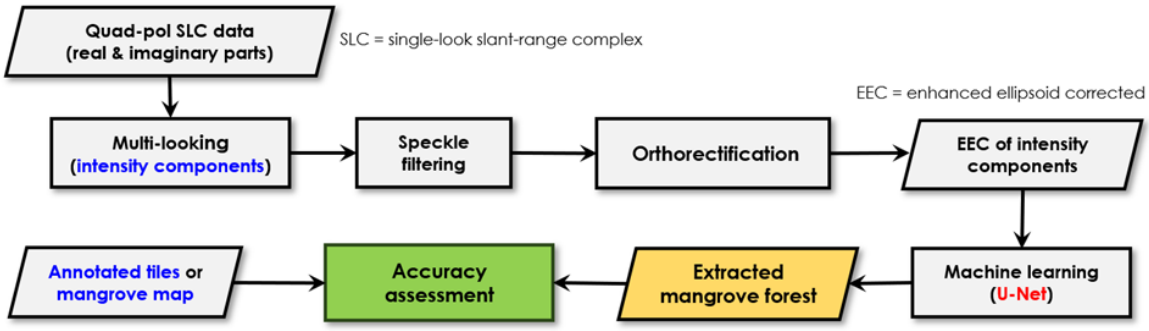

Figure 5: Processing flowchart for mangrove forest extraction

After speckle filtering and orthorectification, the enhanced ellipsoid corrected intensities were employed as inputs into the U-Net model. The results of mangrove forest extraction using 1) multi-polarization with HH, HV and VV intensities versus 2) single-polarization intensity were compared. The aforementioned annotated tiles and a global mangrove map were used for accuracy assessment. The global mangrove forest map (Bunting et al., 2022) over Sungai Pulai study area was downloaded and used as ground truth, since our annotation did not cover this area and the SPMFR is not expected to have change much. The performances of the mangrove forest extraction results were evaluated quantitatively based on overall accuracy, producer accuracy, and user accuracy (see Figure 6).

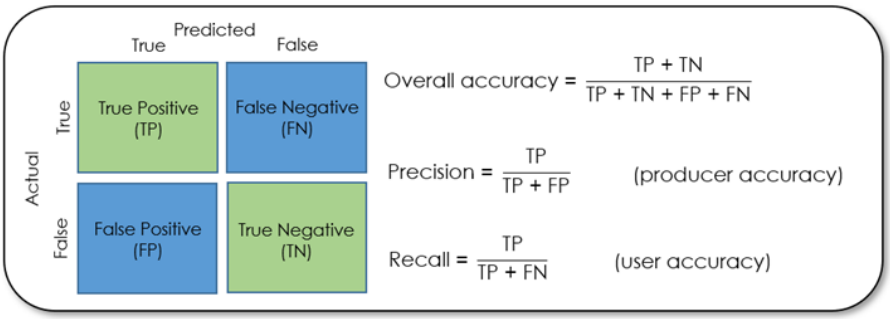

Figure 6: Accuracy assessment

Results and Discussion

a. Mangrove Forest Extraction from CSG Multi-Polarization Data

Based on the trained U-Net model, the predicted mangrove forest extents from the CSG multi-polarization data are shown in Figure 7 to Figure 9. Meanwhile, the computed overall accuracy, producer accuracy (or precision), and user accuracy (or recall) were tabulated in Table 2. As evident from the figures, most of the actual mangrove forests were extracted correctly. By inspecting the extraction results, a little false extraction came from Trees class or Built-up class. Table 2 indicates that all the overall accuracies were greater than or very close to 90%. The user accuracies were all higher than 93%, except for the one over Sungai Pulai (85.4%). The training scene acquired on 26th October 2002 over Matang North gave the expected highest overall accuracy (96.7%) and user accuracy (98.4%). In comparison, the extractions over Matang North had higher overall accuracies than that over Matang South.

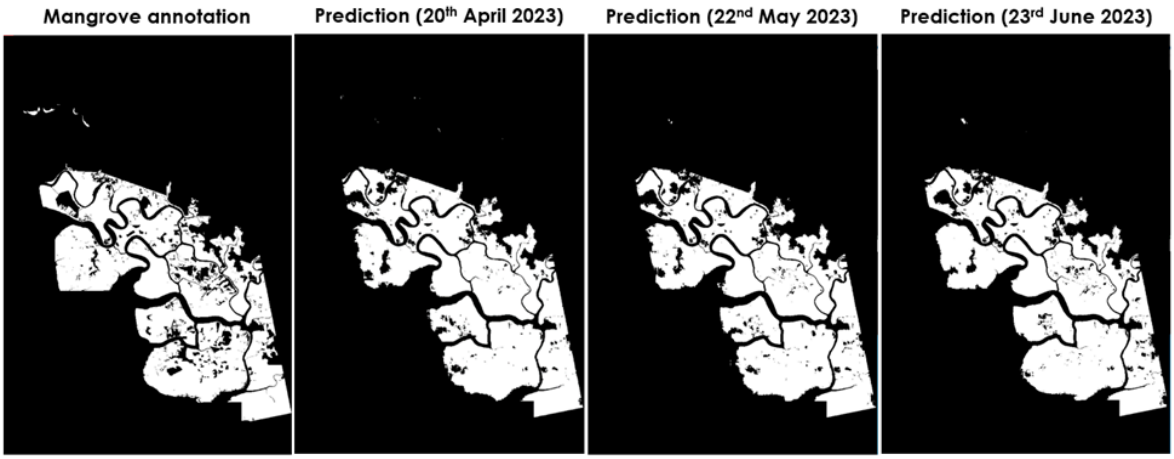

Figure 7: Mangrove forest extraction over Matang North

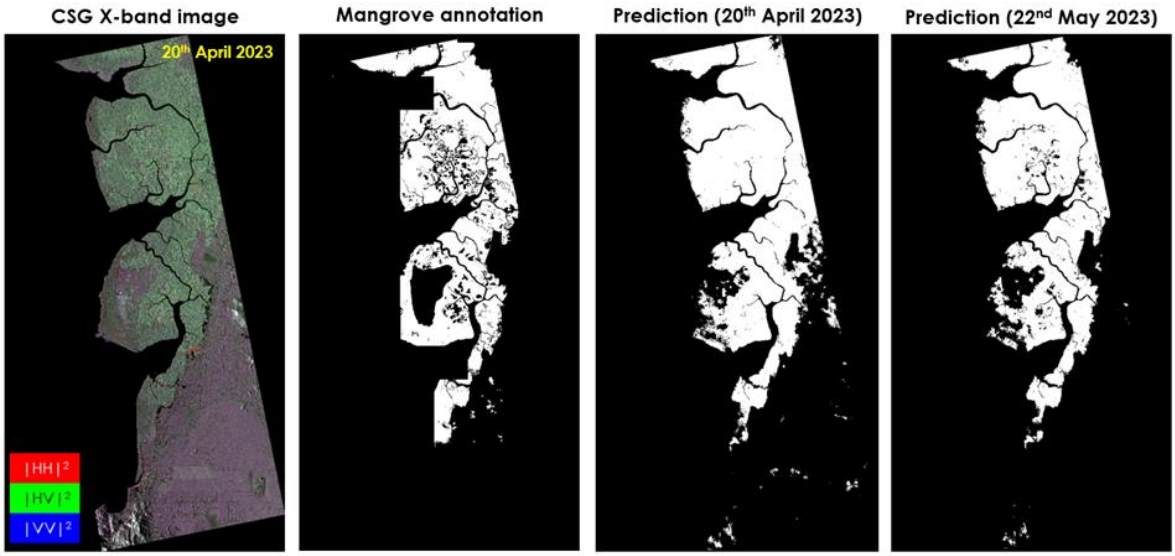

Figure 8: Mangrove forest extraction over Matang South

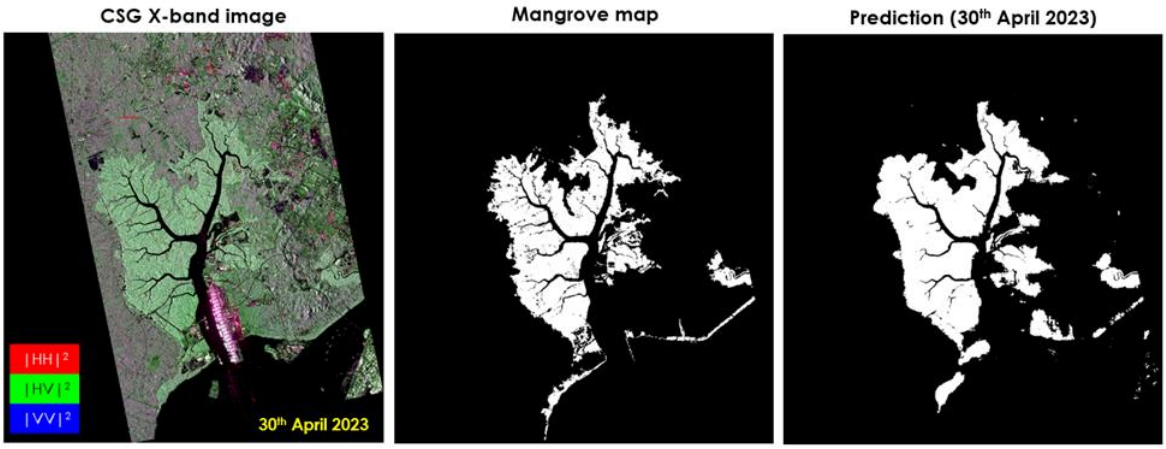

Figure 9: Mangrove forest extraction over Sungai Pulai

Table 2: Accuracy assessment of mangrove extraction from CSG multi-polarization data

Acquisition date	Number of pixels				Overall accuracy (%)	Producer accuracy (%)	User accuracy (%)
	TP	TN	FP	FN			
Matang North							
26th October 2022	6884909	15284650	648540	115498	96.7	91.4	98.4
20th April 2023	7173561	16341895	754100	517960	94.9	90.5	93.3
22nd May 2023	7277334	16198682	897313	414187	94.7	89.0	94.6
23rd June 2023	6516777	14816466	659407	292246	95.7	90.8	95.7
Matang South							
20th April 2023	7141377	4157346	911512	395810	89.6	88.7	94.7
22nd May 2023	6990827	4286104	713886	478104	90.4	907	93.6
Sungai Pulai							
30th April 2023	2922556	24252308	934577	297571	96.4	82.9	85.4

b. Mangrove Forest Extraction from CSG Single-Polarization Data

We also experimented with the mangrove forest extraction from CSG single-polarization data by using the U-Net model. Some of the extraction results are displayed in Figure 10 to Figure 12, where most of the mangrove forests can be extracted correctly from the CSG single-polarization data. These results were further compared quantitatively with those from CSG multi-polarized data. The corresponding overall accuracy, producer accuracy, and user accuracy are listed in Table 3. The HH and VV polarizations produced slightly higher overall accuracies than the HV for the test cases over Matang study site. However, the overall accuracies of Sungai Pulai for the three individual intensities were comparable, between 95% and 96%.

The performance in term of the overall accuracy for all the CSG single-polarization test data is compared in Figure 13. The overall accuracies of mangrove forest extraction from the single-polarization intensity were only slightly lower than those from multi-polarization intensities, i.e., less than 5% in all the CSG test scenes. Moreover, it was found that the overall accuracies for the HH and VV were close to each other. Meanwhile, the overall accuracies for the HV were relatively lower than the HH and VV.

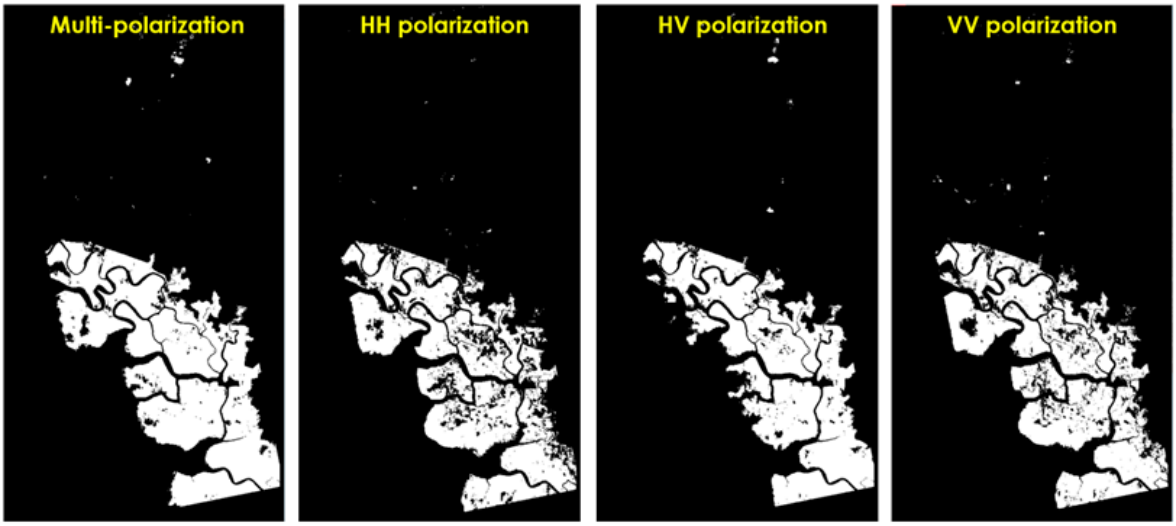

Figure 10: Mangrove forest extraction from CSG scene of Matang North acquired on 20th April 2023

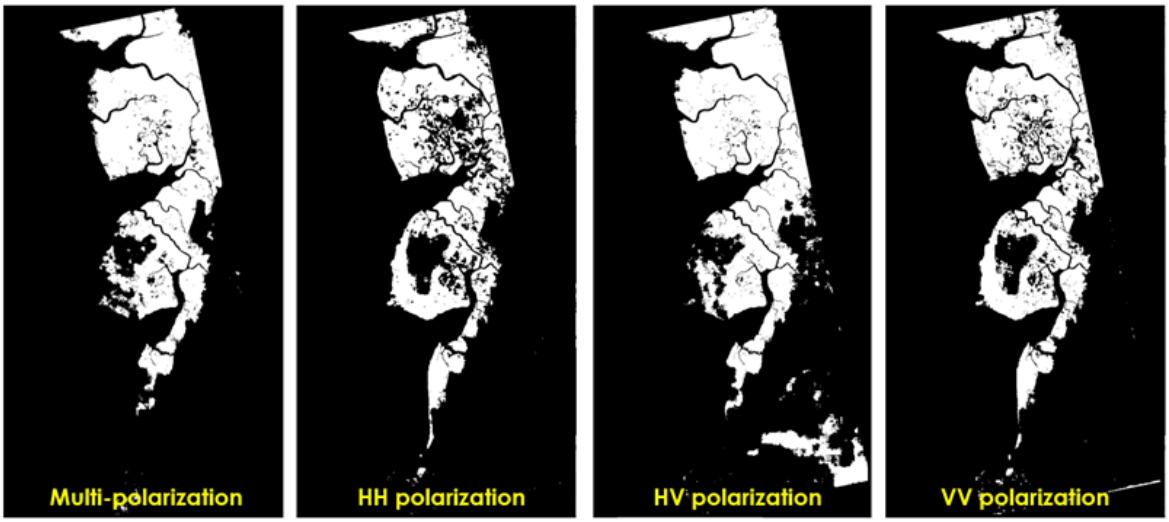

Figure 11: Mangrove forest extraction from CSG scene of Matang South acquired on 22nd May 2023

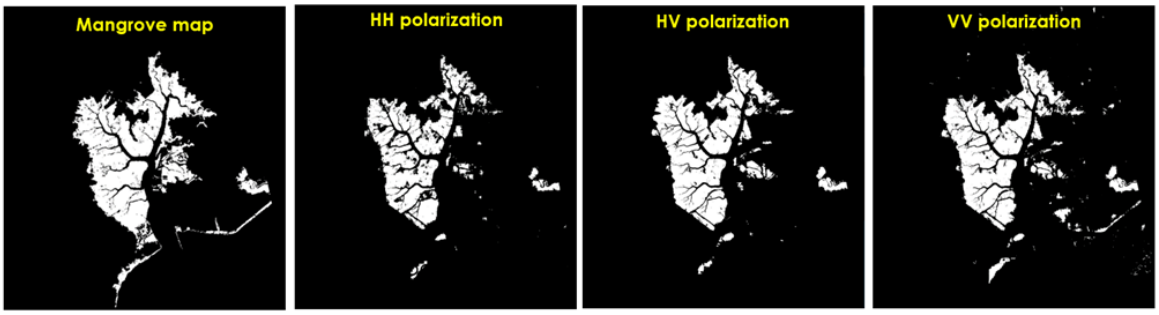

Figure 12: Mangrove forest extraction from CSG scene of Sungai Pulai acquired on 30th April 2023

Table 3: Accuracy assessment of mangrove extraction from CSG data

Band	Number of pixels				Overall accuracy	Producer accuracy	User accuracy
	TP	TN	FP	FN			
Matang North (20th April 2023)							
multi-pol	7173561	16341895	754100	517960	94.9	90.5	93.3
HH	6595046	16783189	312806	1096475	94.3	95.5	85.7
HV	6127667	16402100	693895	1563854	90.9	89.8	79.7
VV	6753146	16617111	478884	938375	94.3	93.4	87.8
Matang South (20th April 2023)							
multi-pol	7141377	4157346	911512	395810	89.6	88.7	94.7
HH	6433435	4830784	238074	1103752	89.4	96.4	85.4
HV	6812117	3408075	1660783	725070	81.1	80.4	90.4
VV	6647272	4594096	474762	889915	89.2	93.3	88.2
Sungai Pulai (30th April 2023)							
multi-pol	2749621	24619352	567533	470506	96.4	82.9	85.4
HH	2528572	24700909	485976	691555	95.9	83.9	78.5
HV	2385205	24755474	431411	834922	95.5	84.7	74.1
VV	2345265	24756884	430001	874862	95.4	84.5	72.8

Note that the overall accuracy, precision and recall are expressed in percentage.

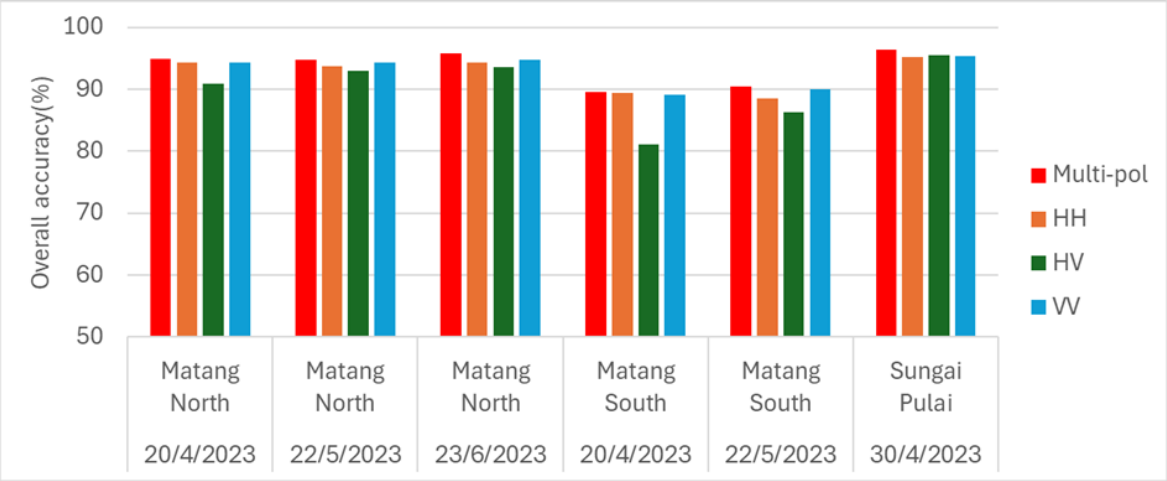

Figure 13: Mangrove forest extraction from CSG data with different acquisition dates

Conclusion

This study examined the capability of COSMO-SkyMed Second Generation X-band SAR for extracting mangrove forests over Matang and Sungai Pulai using the U-Net model. Although the U-Net model was trained with only a small dataset, the multi-polarization data achieved relatively high overall accuracy and user accuracy in mangrove forest extraction. The overall accuracy was as high as 96.7% for the training scene. Furthermore, the overall accuracies in the blind tests also reached 96.4%. By inspecting the extraction results, some confusions between Mangrove and Trees classes were noticed. This observation might be due to similar radar backscattering mechanisms in the X-band imaging for both classes, i.e., mixture of odd-bounce and volume scattering. Moreover, some small patches of mangrove forests along the river side were not well extracted, probably due to insufficient training samples for such a test case. The mangrove extraction results from the CSG single-polarization data indicated that the HH and VV intensities produced higher overall accuracies than the HV intensity, probably due to the limited penetration depth of X band radar. The overall accuracies of mangrove forest extraction from the single-polarization data were slightly lower than those of multi-polarization.

Acknowledgments

The authors acknowledge funding support from the Office for Space Technology and Industry (OSTIn), Singapore Economic Development Board under the Space Technology Development Programme (project reference: S22-02001-STDP). We thank ST Engineering Geo-Insights for inspecting the annotated tiles.

References

Abdel-Hamid, A., Dubovyk, O., Abou El-Magd, I., & Menz, G. (2018). Mapping mangroves extents on the Red Sea coastline in Egypt using polarimetric SAR and high resolution optical remote sensing data. *Sustainability*, *10*(3), 646.

Agenzia Spaziale Italiana (2021). *COSMO-SkyMed Seconda Generazione: System and Products Description* (Doc. No. CE-UOT-2021-002, 217 p.).

Alongi, D. M., Murdiyarso, D., Fourqurean, J. W., Kauffman, J. B., Hutahaean, A., Crooks, S., Lovelock, C. E., Howard, J., Herr, D., Fortes, M., Pidgeon, E., & Wagey, T. (2016). Indonesia's blue carbon: a globally significant and vulnerable sink for seagrass and mangrove carbon. *Wetlands Ecology and Management*, *24*(1), 3-13.

Bunting, P., Rosenqvist, A., Hilarides, L., Lucas, R. M., Thomas, N., Tadono, T., Worthington, T. A., Spalding, M., Murray, N. J., & Rebelo, L. M. (2022). Global mangrove extent change 1996–2020: Global mangrove watch version 3.0. *Remote Sensing*, *14*(15), 3657.

Chen, B., Xiao, X., Li, X., Pan, L., Doughty, R., Ma, J., Dong, J., Qin, Y., Zhao, B., Wu, Z., Sun, R., Lan, G., Zie, G., Clinton N., & Giri, C. (2017). A mangrove forest map of China in 2015: Analysis of time series Landsat 7/8 and Sentinel-1A imagery in Google Earth Engine cloud computing platform. *ISPRS Journal of Photogrammetry and Remote Sensing*, *131*(1), 104-120.

Chong, V. C. (2006). Sustainable utilization and management of mangrove ecosystems of Malaysia. *Aquatic Ecosystem Health & Management*, *9*(2), 249-260.

Donato, D. C., Kauffman, J. B., Murdiyarso, D., Kurnianto, S., Stidham, M., & Kanninen, M. (2011). Mangroves among the most carbon-rich forests in the tropics. *Nature Geoscience*, *4*(5), 293-297.

Friess, D. A., Rogers, K., Lovelock, C. E., Krauss, K. W., Hamilton, S. E., Lee, S. Y., Lucas, R., Primavera, J., Rajkaran, A., & Shi, S. (2019). The state of the world's mangrove forests: past, present, and future. *Annual Review of Environment and Resources*, *44*(1), 89-115.

Ghorbanian, A., Zaghian, S., Asiyabi, R. M., Amani, M., Mohammadzadeh, A., & Jamali, S. (2021). Mangrove ecosystem mapping using Sentinel-1 and Sentinel-2 satellite images and random forest algorithm in Google Earth Engine. *Remote Sensing*, *13*(13), 2565.

Hamdan, O., Khali Aziz, H., & Mohd Hasmadi, I (2014). L-band ALOS PALSAR for biomass estimation of Matang Mangroves, Malaysia. *Remote Sensing of Environment*, *155*(1), 69-78.

Hamilton, S. E., & Friess, D. A. (2018). Global carbon stocks and potential emissions due to mangrove deforestation from 2000 to 2012. *Nature Climate Change*, *8*(3), 240-244.

Islam, M. A., Billah, Md. M., Idris, M. H., Bhuiyan, Md. K. A., & Kamal, A. H. M. (2024). Mangroves of Malaysia: a comprehensive review on ecosystem functions, services, restorations, and potential threats of climate change. *Hydrobiologia*, *851*, 1841-1871.

Jhonnerie, R., Siregar, V. P., Nababan, B., Prasetyo, L. B., & Wouthuyzen, S. (2015). Random forest classification for mangrove land cover mapping using Landsat 5 TM and ALOS PALSAR imageries. *Procedia Environmental Sciences*, *24*(1), 215-221.

Kanniah, K. D., Kang, C. S., Sharma, S, & Amir, A. A. (2021). Remote sensing to study mangrove fragmentation and its impacts on leaf area index and gross primary productivity in the south of Peninsular Malaysia. *Remote Sensing*, *13*, 1427.

Kovacs, J. M., Jiao, X., Flores-de-Santiago, F., Zhang, C., & Flores-Verdugo, F. (2013). Assessing relationships between Radarsat-2 C-band and structural parameters of a degraded mangrove forest. *International Journal of Remote Sensing*, *34*(20), 7002-7019.

Lee, K. Y., Hou, C. G., Liew, S. C., & Kwoh, L. K. (2021). Gravitation-based bilateral filtering of ALOS-2 PALSAR-2 polarimetric data. *2021 IEEE International Geoscience and Remote Sensing Symposium*, 4747-4750.

Liu, X., Fatoyinbo, T. E., Thomas, N. M., Guan, W. W., Zhan, Y., Mondal, P., Lagomasino, D., Simard, M., Trettin, C. C., Deo, R., & Barenblitt, A. (2021). Large-scale high-resolution coastal mangrove forests mapping across West Africa with machine learning ensemble and satellite big data. *Frontiers in Earth Science*, *8*(1), 560933.

Lucas, R., Otero, V., Van De Kerchove, R., Lagomasino, D., Satyanarayana, B., Fatoyinbo, T., & Dahdouh-Guebas, F. (2021). Monitoring Matang's Mangroves in Peninsular Malaysia through earth observations: A globally relevant approach. *Land Degradation & Development*, *32*, 354-373.

Lucas, R., Rebelo, L. M., Fatoyinbo, L., Rosenqvist, A., Itoh, T., Shimada, M., Simard, M., Souza-Filho, P. W., Thomas, N., Trettin, C., Accad, A., Carreiras, J., & Hilarides, L. (2014). Contribution of L-band SAR to systematic global mangrove monitoring. *Marine and Freshwater Research*, *65*(7), 589-603.

Mohd Hasmadi, I., Pakhriazad, H. Z., & Norlida, K. (2011). Remote sensing for mapping RAMSAR heritage site at Sungai Pulai Mangrove Forest Reserve, Johor, Malaysia. *Sains Malaysiana, 40*(2), 83–88.

Murdiyarso, D., Purbopuspito, J., Kauffman, J. B., Warren, M. W., Sasmito, S. D., Donato, D. C., Manuri, S., Krisnawati, H., Taberima, S. & Kurnianto, S. (2015). The potential of Indonesian mangrove forests for global climate change mitigation. *Nature Climate Change*, *5*(12), 1089-1092.

Ong, J. E., & Gong, W.K. (2013). *Structure, Function and Management of Mangrove Ecosystems*. International Society for Mangrove Ecosystems and International Tropical Timber Organization.

Pham, T. D., Yokoya, N., Bui, D. T., Yoshino, K., & Friess, D. A. (2019). Remote sensing approaches for monitoring mangrove species, structure, and biomass: Opportunities and challenges. *Remote Sensing, 11*(3), 230.

Proisy, C., Mougin, E., Fromard, F., & Karam, M. A. (2000). Interpretation of polarimetric radar signatures of mangrove forests. *Remote Sensing of Environment, 71*, 56-66.

Romañach, S. S., DeAngelis, D. L., Koh, H. L., Li, Y., Teh, S. Y., Raja Barizan, R. S., & Zhai, L. (2018). Conservation and restoration of mangroves: Global status, perspectives, and prognosis. *Ocean and Coastal Management, 154*, 72-82.

Ronneberger, O., Fischer, P., & Brox, T. (2015). U-Net: Convolutional networks for biomedical image segmentation. *arXiv*. https://arxiv.org/abs/1505.04597

Sharifi, A., Felegari, S., & Tariq, A. (2022). Mangrove forests mapping using Sentinel-1 and Sentinel-2 satellite images. *Arabian Journal of Geosciences, 15*(20), 1593.

Small, D., & Schubert, A. (2008). *Guide to ASAR Geocoding* (Reference No. RSL-ASAR-GC-AD). University of Zurich.

Solórzano, J. V., Mas, J. F., Gao, Y., & Gallardo-Cruz, J. A. (2021). Land use land cover classification with U-net: Advantages of combining Sentinel-1 and Sentinel-2 imagery. *Remote Sensing*, *13*(18), 3600.

Vu, T. D., Takeuchi, W., & Van, N. A. (2014). Carbon stock calculating and forest change assessment toward REDD+ activities for the mangrove forest in Vietnam. *Transactions of the Japan Society for Aeronautical and Space Sciences, Aerospace Technology Japan*, *12*(29), Pn_23-Pn_31.

Wang, L., Jia, M., Yin, D., & Tian, J. (2019). A review of remote sensing for mangrove forests: 1956–2018. *Remote Sensing of Environment*, *231*(1), 111223.

Whitmore, T. C. (1984). *Tropical Rain Forests of the Far East* (2nd ed.). Oxford University Press.